

¹ Power laws and critical fragmentation in global forests

² Leonardo A. Saravia^{1 3}, Santiago R. Doyle¹, Ben Bond-Lamberty²

³ 1. Instituto de Ciencias, Universidad Nacional de General Sarmiento, J.M. Gutierrez 1159 (1613), Los
⁴ Polvorines, Buenos Aires, Argentina.

⁵ 2. Pacific Northwest National Laboratory, Joint Global Change Research Institute at the University of
⁶ Maryland–College Park, 5825 University Research Court #3500, College Park, MD 20740, USA

⁷ 3. Corresponding author e-mail: lsaravia@ungs.edu.ar

⁸ **Keywords:** Forest fragmentation, early warning signals, percolation, power-laws, MODIS, critical transitions

⁹ **Running title:** Critical fragmentation in global forest

¹⁰ Word count Abstract: 144

¹¹ Word count main text: 5813

¹² type of article: Letters

¹³ Number of references: 101

¹⁴ Number of figures and tables: 5

¹⁵ Statement of authorship: LAS designed the study, SRD LAS performed modelling work, BBL review methods,
¹⁶ and LAS SRD BBL wrote the manuscript

¹⁷ Data accessibility statement: all the raw data is from public repositories, the data supporting the results is
¹⁸ archived at figshare public repository and the data DOI is included at in the article..

¹⁹ **Abstract**

²⁰ The replacement of forest areas with human-dominated landscapes usually leads to fragmentation, altering
²¹ the structure and function of the forest. Here we studied the dynamics of forest patch sizes at a global level,
²² examining signals of a critical transition from an unfragmented to a fragmented state, using the MODIS
²³ vegetation continuous field. We defined wide regions of connected forest across continents and big islands,
²⁴ and combined five criteria, including the distribution of patch sizes and the fluctuations of the largest patch
²⁵ over the last sixteen years, to evaluate the closeness of each region to a fragmentation threshold. Regions with
²⁶ the highest deforestation rates—South America, Southeast Asia, Africa—all met these criteria and may thus
²⁷ be near a critical fragmentation threshold. This implies that if current forest loss rates are maintained, wide
²⁸ continental areas could suddenly fragment, triggering extensive species loss and degradation of ecosystems
²⁹ services.

30 Introduction

31 Forests are one of the most important biomes on earth, providing habitat for a large proportion of species
32 and contributing extensively to global biodiversity (Crowther *et al.* 2015). In the previous century, human
33 activities have influenced global bio-geochemical cycles (Bonan 2008; Canfield *et al.* 2010), with one of
34 the most dramatic changes being the replacement of 40% of Earth's formerly biodiverse land areas with
35 landscapes that contain only a few species of crop plants, domestic animals and humans (Foley *et al.* 2011).

36 These local changes have accumulated over time and now constitute a global forcing (Barnosky *et al.* 2012).
37 Another global scale forcing that is tied to habitat destruction is fragmentation, which is defined as the
38 division of a continuous habitat into separated portions that are smaller and more isolated. Fragmentation
39 produces multiple interwoven effects: reductions of biodiversity between 13% and 75%, decreasing forest
40 biomass, and changes in nutrient cycling (Haddad *et al.* 2015). The effects of fragmentation are not only
41 important from an ecological point of view but also that of human activities, as ecosystem services are deeply
42 influenced by the level of landscape fragmentation (Rudel *et al.* 2005; Angelsen 2010; Mitchell *et al.* 2015).

43 Ecosystems have complex interactions between species and present feedbacks at different levels of organi-
44 zation (Gilman *et al.* 2010), and external forcings can produce abrupt changes from one state to another,
45 called critical transitions (Scheffer *et al.* 2009). Such 'critical' transitions have been detected mostly at local
46 scales (Drake & Griffen 2010; Carpenter *et al.* 2011), but the accumulation of changes in local communities
47 that overlap geographically can propagate and theoretically cause an abrupt change of the entire system at
48 larger scales (Barnosky *et al.* 2012).

49 Complex systems can experience two general classes of critical transitions (Solé 2011). In so-called first-
50 order transitions, a catastrophic regime shift that is mostly irreversible occurs because of the existence of
51 alternative stable states (Scheffer *et al.* 2001). This class of transitions is suspected to be present in a variety
52 of ecosystems such as lakes, woodlands, coral reefs (Scheffer *et al.* 2001), semi-arid grasslands (Bestelmeyer
53 *et al.* 2011), and fish populations (Vasilakopoulos & Marshall 2015). They can be the result of positive
54 feedback mechanisms (Villa Martín *et al.* 2015); for example, fires in some forest ecosystems were more
55 likely to occur in previously burned areas than in unburned places (Kitzberger *et al.* 2012).

56 The other class of critical transitions are continuous or second order transitions (Solé & Bascompte 2006). In
57 these cases, there is a narrow region where the system suddenly changes from one domain to another, with
58 the change being continuous and in theory reversible. This kind of transitions were suggested to be present
59 in tropical forests (Pueyo *et al.* 2010; Taubert *et al.* 2018), semi-arid mountain ecosystems (McKenzie
60 & Kennedy 2012), and tundra shrublands (Naito & Cairns 2015). The transition happens at a critical

61 point where we can observe a distinctive spatial pattern: scale-invariant fractal structures characterized by
62 power law patch distributions (Stauffer & Aharony 1994). There are several processes that can convert a
63 catastrophic transition to a second order transition (Villa Martín *et al.* 2015). These include stochasticity,
64 such as demographic fluctuations, spatial heterogeneities, and/or dispersal limitation. All these components
65 are present in forest around the globe (Seidler & Plotkin 2006; Filotas *et al.* 2014; Fung *et al.* 2016),
66 and thus continuous transitions might be more probable than catastrophic transitions. Moreover, there is
67 some evidence of recovery in some systems that supposedly suffered an irreversible transition produced by
68 overgrazing (Zhang *et al.* 2005; Bestelmeyer *et al.* 2013) and desertification (Allington & Valone 2010).

69 The spatial phenomena observed in continuous critical transitions deal with connectivity, a fundamental
70 property of general systems and ecosystems from forests (Ochoa-Quintero *et al.* 2015) to marine ecosystems
71 (Leibold & Norberg 2004) and the whole biosphere (Lenton & Williams 2013). When a system goes from a
72 fragmented to a connected state we say that it percolates (Solé 2011). Percolation implies that there is a
73 path of connections that involve the whole system. Thus we can characterize two domains or phases: one
74 dominated by short-range interactions where information cannot spread, and another in which long-range
75 interactions are possible and information can spread over the whole area. (The term “information” is used
76 in a broad sense and can represent species dispersal or movement.) Thus, there is a critical “percolation
77 threshold” between the two phases, and the system could be driven close to or beyond this point by an
78 external force; climate change and deforestation are the main forces that could be the drivers of such a phase
79 change in contemporary forests (Bonan 2008; Haddad *et al.* 2015). There are several applications of this
80 concept in ecology: species’ dispersal strategies are influenced by percolation thresholds in three-dimensional
81 forest structure (Solé *et al.* 2005), and it has been shown that species distributions also have percolation
82 thresholds (He & Hubbell 2003). This implies that pushing the system below the percolation threshold could
83 produce a biodiversity collapse (Bascompte & Solé 1996; Solé *et al.* 2004; Pardini *et al.* 2010); conversely,
84 being in a connected state (above the threshold) could accelerate the invasion of the forest into prairie (Loehle
85 *et al.* 1996; Naito & Cairns 2015).

86 One of the main challenges with systems that can experience critical transitions—of any kind—is that the
87 value of the critical threshold is not known in advance. In addition, because near the critical point a small
88 change can precipitate a state shift in the system, they are difficult to predict. Several methods have been
89 developed to detect if a system is close to the critical point, e.g. a deceleration in recovery from perturbations,
90 or an increase in variance in the spatial or temporal pattern (Hastings & Wysham 2010; Carpenter *et al.*
91 2011; Boettiger & Hastings 2012; Dai *et al.* 2012).

92 The existence of a critical transition between two states has been established for forest at a global scale in

93 different works (Hirota *et al.* (2011); Staal *et al.* (2016); Wuyts *et al.* (2017)). It is generally believed that
94 this constitutes a first order catastrophic transition. The regions where forest can grow are not distributed
95 homogeneously, as there are demographic fluctuations in forest growth and disturbances produced by human
96 activities. All these factors imply that if these were first order transitions they will be converted or observed
97 as second order continuous transitions (Villa Martín *et al.* 2014, 2015). From this basis, we applied indices
98 derived from second-order transitions to global forest cover dynamics.

99 In this study, our objective is to look for evidence that forests around the globe are near continuous critical
100 points that represent a fragmentation threshold. We use the framework of percolation to first evaluate if
101 forest patch distribution at a continental scale is described by a power law distribution and then examine
102 the fluctuations of the largest patch. The advantage of using data at a continental scale is that for very large
103 systems the transitions are very sharp (Solé 2011) and thus much easier to detect than at smaller scales,
104 where noise can mask the signals of the transition.

105 Methods

106 Study areas definition

107 We analyzed mainland forests at a continental scale, covering the whole globe, by delimiting land areas with
108 a near-contiguous forest cover, separated with each other by large non-forested areas. Using this criterion,
109 we delimited the following forest regions. In America, three regions were defined: South America temperate
110 forest (SAT), subtropical and tropical forest up to Mexico (SAST), and USA and Canada forest (NA). Europe
111 and North Asia were treated as one region (EUAS). The rest of the delimited regions were South-east Asia
112 (SEAS), Africa (AF), and Australia (OC). We also included in the analysis islands larger than 10^5km^2 . We
113 applied this criterion to delimit regions because we based our study on percolation theory that assumes some
114 kind of connectivity in the study area (Appendix Table S2, figure S1-S6).

115 Forest patch distribution

116 We studied forest patch distribution in each defined area from 2000 to 2015 using the MODerate-resolution
117 Imaging Spectroradiometer (MODIS) Vegetation Continuous Fields (VCF) Tree Cover dataset version 051
118 (DiMiceli *et al.* 2015). This dataset is produced at a global level with a 231-m resolution, from 2000 onwards
119 on an annual basis, the last available year was 2015. There are several definitions of forest based on percent
120 tree cover (Sexton *et al.* 2015); we choose a range from 20% to 40% threshold in 5% increments to convert

the percentage tree cover to a binary image of forest and non-forest pixels. This range is centered in the definition used by the United Nations' International Geosphere-Biosphere Programme (Belward 1996), and studies of global fragmentation (Haddad *et al.* 2015) and includes the range used in other studies of critical transitions (Xu *et al.* 2016). Using this range we try to avoid the errors produced by low discrimination of MODIS VCF between forest and dense herbaceous vegetation at low forest cover and the saturation of MODIS VCF in dense forests (Sexton *et al.* 2013). We repeat all the analysis for this set of thresholds, except in some specific cases described below. Patches of contiguous forest were determined in the binary image by grouping connected forest pixels using a neighborhood of 8 forest units (Moore neighborhood). The MODIS VCF product defines the percentage of tree cover by pixel but does not discriminate the type of trees so besides natural forest it includes plantations of tree crops like rubber, oil palm, eucalyptus and other managed stands (Hansen *et al.* 2014).

Percolation theory

A more in-depth introduction to percolation theory can be found elsewhere (Stauffer & Aharony 1994) and a review from an ecological point of view is available (Oborny *et al.* 2007). Here, to explain the basic elements of percolation theory we formulate a simple model: we represent our area of interest by a square lattice and each site of the lattice can be occupied—e.g. by forest—with a probability p . The lattice will be more occupied when p is greater, but the sites are randomly distributed. We are interested in the connection between sites, so we define a neighborhood as the eight adjacent sites surrounding any particular site. The sites that are neighbors of other occupied sites define a patch. When there is a patch that connects the lattice from opposite sides, it is said that the system percolates. When p is increased from low values, a percolating patch suddenly appears at some value of p called the critical point p_c .

Thus percolation is characterized by two well-defined phases: the unconnected phase when $p < p_c$ (called subcritical in physics), in which species cannot travel far inside the forest, as it is fragmented; in a general sense, information cannot spread. The second is the connected phase when $p > p_c$ (supercritical), species can move inside a forest patch from side to side of the area (lattice), i.e. information can spread over the whole area. Near the critical point, several scaling laws arise: the structure of the patch that spans the area is fractal, the size distribution of the patches is power-law, and other quantities also follow power-law scaling (Stauffer & Aharony 1994).

The value of the critical point p_c depends on the geometry of the lattice and on the definition of the neighborhood, but other power-law exponents only depend on the lattice dimension. Close to the critical

151 point, the distribution of patch sizes is:

152 (1) $n_s(p_c) \propto s^{-\alpha}$

153 where $n_s(p)$ is the number of patches of size s . The exponent α does not depend on the details of the
154 model and it is called universal (Stauffer & Aharony 1994). These scaling laws can be applied to landscape
155 structures that are approximately random, or at least only correlated over short distances (Gastner *et al.*
156 2009). In physics, this is called “isotropic percolation universality class”, and corresponds to an exponent
157 $\alpha = 2.05495$. If we observe that the patch size distribution has another exponent it will not belong to this
158 universality class and some other mechanism should be invoked to explain it. Percolation thresholds can also
159 be generated by models that have some kind of memory (Hinrichsen 2000; Ódor 2004): for example, a patch
160 that has been exploited for many years will recover differently than a recently deforested forest patch. In
161 this case, the system could belong to a different universality class, or in some cases, there is no universality,
162 in which case the value of α will depend on the parameters and details of the model (Corrado *et al.* 2014).

163 To illustrate these concepts, we conducted simulations with a simple forest model with only two states: forest
164 and non-forest. This type of model is called a “contact process” and was introduced for epidemics (Harris
165 1974) but has many applications in ecology (Solé & Bascompte 2006; Gastner *et al.* 2009). A site with forest
166 can become extinct with probability e , and produce another forest site in a neighborhood with probability
167 c . We use a neighborhood defined by an isotropic power law probability distribution. We defined a single
168 control parameter as $\lambda = c/e$ and ran simulations for the subcritical fragmentation state $\lambda < \lambda_c$, with $\lambda = 2$,
169 near the critical point for $\lambda = 2.5$, and for the supercritical state with $\lambda = 5$ (see supplementary data, gif
170 animations).

171 Patch size distributions

172 We fitted the empirical distribution of forest patches calculated for each of the thresholds on the range we
173 previously mentioned. We used maximum likelihood (Goldstein *et al.* 2004; Clauset *et al.* 2009) to fit four
174 distributions: power-law, power-law with exponential cut-off, log-normal, and exponential. We assumed
175 that the patch size distribution is a continuous variable that was discretized by the remote sensing data
176 acquisition procedure.

177 The power-law distribution needs a lower bound for its scaling behavior. This lower bound is also estimated
178 from the data by maximizing the Kolmogorov-Smirnov (KS) statistic, computed by comparing the empirical
179 and fitted cumulative distribution functions (Clauset *et al.* 2009). For the log-normal model, we constrain
180 the values of the μ parameter to positive values, this parameter controls the mode of the distribution and

181 when is negative most of the probability density of the distribution lies outside the range of the forest patch
182 size data (Limpert *et al.* 2001).

183 To select the best model we calculated corrected Akaike Information Criteria (AIC_c) and Akaike weights
184 for each model (Burnham & Anderson 2002). Akaike weights (w_i) are the weight of evidence in favor of
185 model i being the actual best model given that one of the N models must be the best model for that set of
186 N models. Additionally, we computed a likelihood ratio test (Vuong 1989; Clauset *et al.* 2009) of the power
187 law model against the other distributions. We calculated bootstrapped 95% confidence intervals (Crawley
188 2012) for the parameters of the best model, using the bias-corrected and accelerated (BCa) bootstrap (Efron
189 & Tibshirani 1994) with 10000 replications.

190 Largest patch dynamics

191 The largest patch is the one that connects the highest number of sites in the area. This has been used
192 extensively to indicate fragmentation (Gardner & Urban 2007; Ochoa-Quintero *et al.* 2015) and the size of
193 the largest patch S_{max} has been studied in relation to percolation phenomena (Stauffer & Aharony 1994;
194 Bazant 2000; Botet & Ploszajczak 2004) but is seldom used in ecological studies (for an exception see Gastner
195 *et al.* (2009)). When the system is in a connected state ($p > p_c$) the landscape is almost insensitive to the
196 loss of a small fraction of forest, but close to the critical point a minor loss can have important effects (Solé
197 & Bascompte 2006; Oborny *et al.* 2007), because at this point the largest patch will have a filamentary
198 structure, i.e. extended forest areas will be connected by thin threads. Small losses can thus produce large
199 fluctuations.

200 One way to evaluate the fragmentation of the forest is to calculate the proportion of the largest patch against
201 the total area (Keitt *et al.* 1997). The total area of the regions we are considering (Appendix S4, figures
202 S1-S6) may not be the same as the total area that the forest could potentially occupy, and thus a more
203 accurate way to evaluate the weight of S_{max} is to use the total forest area, which can be easily calculated
204 by summing all the forest pixels. We calculate the proportion of the largest patch for each year, dividing
205 S_{max} by the total forest area of the same year: $RS_{max} = S_{max} / \sum_i S_i$. This has the effect of reducing the
206 S_{max} fluctuations produced due to environmental or climatic changes influences in total forest area. When
207 the proportion RS_{max} is large (more than 60%) the largest patch contains most of the forest so there are
208 fewer small forest patches and the system is probably in a connected phase. Conversely, when it is low (less
209 than 20%), the system is probably in a fragmented phase (Saravia & Momo 2018). To define if a region will
210 be in a connected or unconnected state we used the RS_{max} of the highest (i.e., most conservative) threshold

211 of 40%, that represents the densest area of forest within our chosen range. We assume that there are two
212 alternative states for the critical transition—the forest could be fragmented or unfragmented. If RS_{max} is
213 a good indicator of the fragmentation state of the forest its distribution of frequencies should be bimodal
214 (Bestelmeyer *et al.* 2011), so we apply the Hartigan’s dip test that measures departures from unimodality
215 (Hartigan & Hartigan 1985).

216 To evaluate if the system is near a critical transition, we calculate the fluctuations of the largest patch
217 $\Delta S_{max} = S_{max}(t) - \langle S_{max} \rangle$, using the same formula for RS_{max} . To characterize fluctuations we fitted
218 three empirical distributions: power-law, log-normal, and exponential, using the same methods described
219 previously. We expect that large fluctuations near a critical point have heavy tails (log-normal or power-law)
220 and that fluctuations far from a critical point have exponential tails, corresponding to Gaussian processes
221 (Rooij *et al.* 2013). We also apply likelihood ratio test explained previously (Vuong 1989; Clauset *et al.*
222 2009); if the p-values obtained to compare the best distribution against the others are not significant we
223 concluded that there is not enough data to decide which is the best model. We generated animated maps
224 showing the fluctuations of the two largest patches at 30% threshold, to aid in the interpretations of the
225 results.

226 A robust way to detect if the system is near a critical transition is to analyze the increase in variance of the
227 density (Benedetti-Cecchi *et al.* 2015)—in our case ‘density’ is the total forest cover divided by the area.
228 It has been demonstrated that the variance increase in density appears when the system is very close to
229 the transition (Corrado *et al.* 2014), and thus practically it does not constitute an early warning indicator.
230 An alternative is to analyze the variance of the fluctuations of the largest patch ΔS_{max} : the maximum is
231 attained at the critical point but a significant increase occurs well before the system reaches the critical point
232 (Corrado *et al.* 2014; Saravia & Momo 2018). In addition, before the critical fragmentation, the skewness
233 of the distribution of ΔS_{max} should be negative, implying that fluctuations below the average are more
234 frequent. We characterized the increase in the variance using quantile regression: if variance is increasing
235 the slopes of upper or/and lower quartiles should be positive or negative.

236 All statistical analyses were performed using the GNU R version 3.3.0 (R Core Team 2015), to fit the
237 distributions of patch sizes we used the Python package powerlaw (Alstott *et al.* 2014). For the quantile
238 regressions, we used the R package quantreg (Koenker 2016). Image processing was done in MATLAB
239 r2015b (The Mathworks Inc.). The complete source code for image processing and statistical analysis and
240 the patch size data files are available at figshare <http://dx.doi.org/10.6084/m9.figshare.4263905>.

²⁴¹ **Results**

²⁴² Figure 1 shows an example of the distribution of the biggest 200 patches for years 2000 and 2014. This
²⁴³ distribution is highly variable; the biggest patch usually maintains its spatial location, but sometimes it
²⁴⁴ breaks and then big temporal fluctuations in its size are observed, as we will analyze below. Smaller patches
²⁴⁵ can merge or break more easily so they enter or leave the list of 200, and this is why there is a color change
²⁴⁶ across years.

²⁴⁷ The power law distribution was selected as the best model in 99% of the cases (Figure S7). In a small
²⁴⁸ number of cases (1%), the power law with exponential cutoff was selected, but the value of the parameter α
²⁴⁹ was similar by ± 0.03 to the pure power law (Table S1 and model fit data table). Additionally, the patch size
²⁵⁰ where the exponential tail begins is very large, and thus we used the power law parameters for these cases
²⁵¹ (region EUAS3, SAST2). In finite-size systems, the favored model should be the power law with exponential
²⁵² cut-off because the power-law tails are truncated to the size of the system (Stauffer & Aharony 1994). This
²⁵³ implies that differences between the two kinds of power law models should be small. We observe this effect:
²⁵⁴ when the pure power-law model is selected as the best model the likelihood ratio test shows that in 64% of
²⁵⁵ the cases the differences with power law with exponential cutoff are not significant ($p\text{-value} > 0.05$); in these
²⁵⁶ cases the differences between the fitted α for both models are less than 0.001. Instead, the likelihood ratio
²⁵⁷ test clearly differentiates the power law model from the exponential model (100% cases $p\text{-value} < 0.05$), and
²⁵⁸ the log-normal model (90% cases $p\text{-value} < 0.05$).

²⁵⁹ The global mean of the power-law exponent α is 1.967 and the bootstrapped 95% confidence interval is
²⁶⁰ 1.964 - 1.970. The global values for each threshold are different, because their confidence intervals do not
²⁶¹ overlap, and their range goes from 1.90 to 2.01 (Table S1). Analyzing the biggest regions (Figure 1, Table
²⁶² S2) the northern hemisphere regions (EUAS1 & NA1) have similar values of α (1.97, 1.98), pantropical areas
²⁶³ have different α with greatest values for South America (SAST1, 2.01) and in descending order Africa (AF1,
²⁶⁴ 1.946) and Southeast Asia (SEAS1, 1.895). With greater α the fluctuations of patch sizes are lower and vice
²⁶⁵ versa (Newman 2005).

²⁶⁶ We calculated the total areas of forest and the largest patch S_{max} by year for different thresholds, and as
²⁶⁷ expected these two values increase for smaller thresholds (Table S3). We expect fewer variations in the
²⁶⁸ largest patch relative to total forest area RS_{max} (Figure S9); in ten cases it stayed near or higher than 60%
²⁶⁹ (EUAS2, NA5, OC2, OC3, OC4, OC5, OC6, OC8, SAST1, SAT1) over the 25-35 range or more. In four
²⁷⁰ cases it stayed around 40% or less, at least over the 25-30% range (AF1, EUAS3, OC1, SAST2), and in six
²⁷¹ cases there is a crossover from more than 60% to around 40% or less (AF2, EUAS1, NA1, OC7, SEAS1,

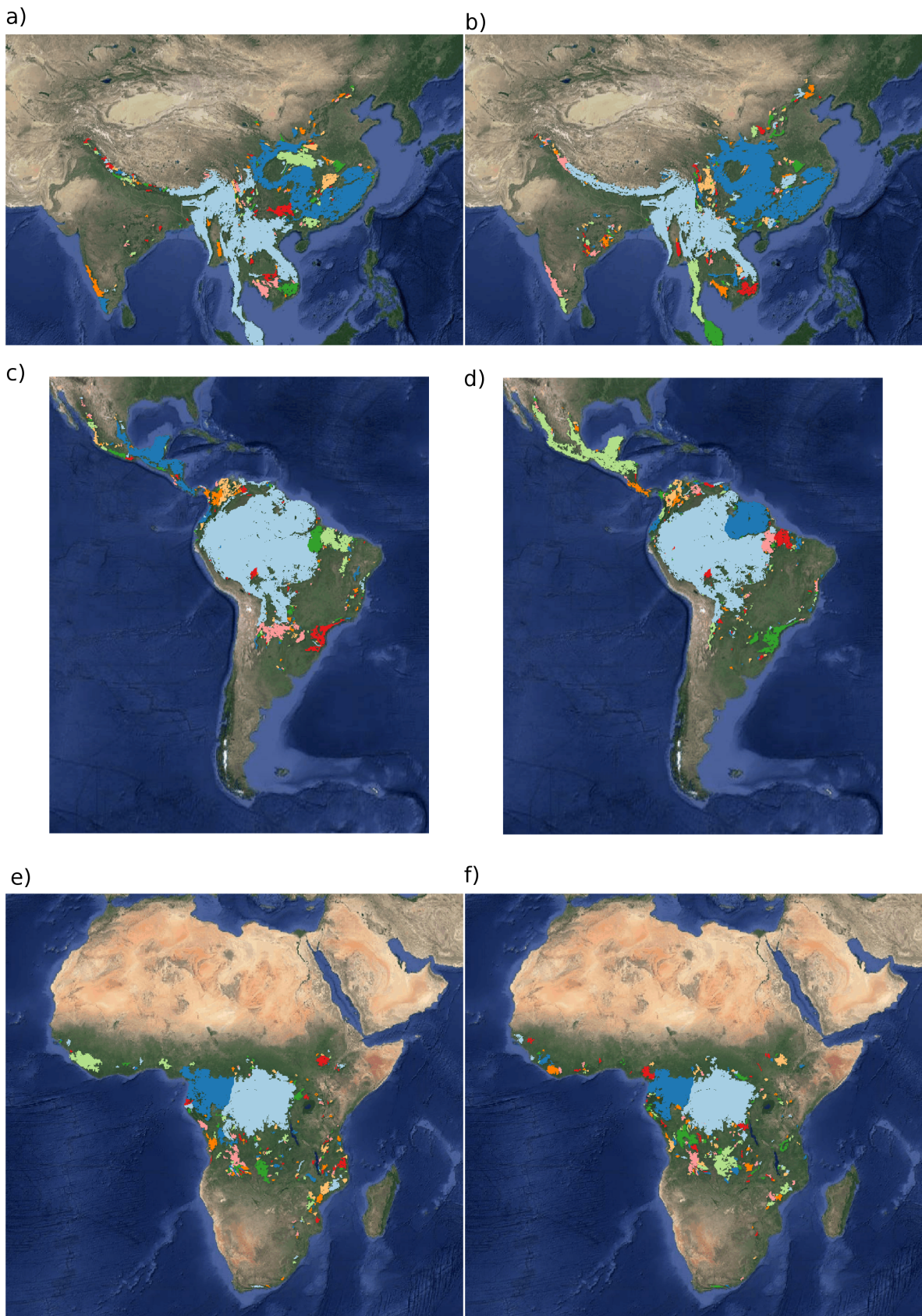


Figure 1: Forest patch distributions for continental regions for the years 2000 and 2014. The images are the 200 biggest patches, shown at a coarse pixel scale of 2.5 km. The regions are: a) & b) southeast Asia; c) & d) South America subtropical and tropical and e) & f) Africa mainland, for the years 2000 and 2014 respectively. The color palette was chosen to discriminate different patches and does not represent patch size.

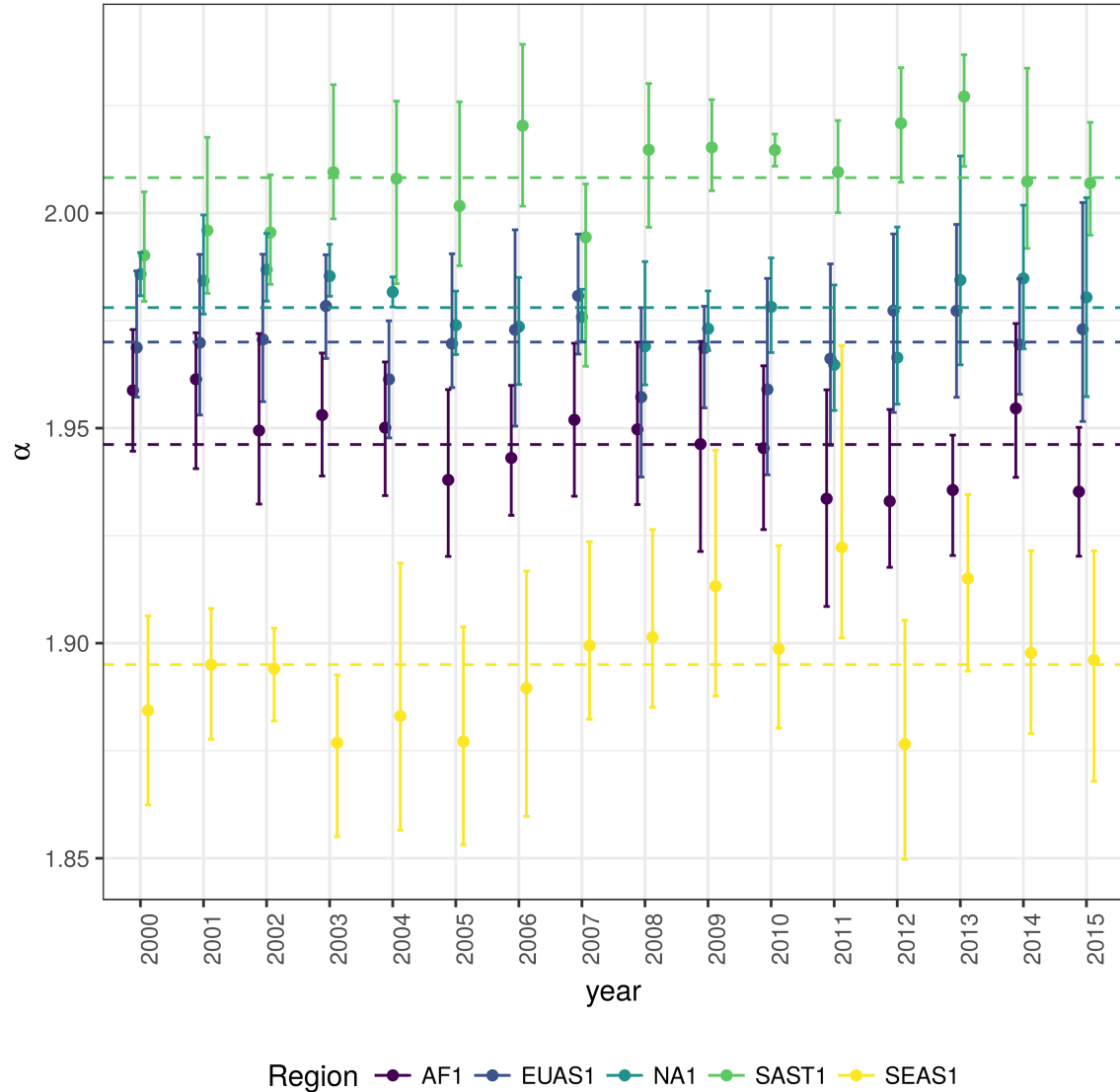


Figure 2: Power law exponents (α) of forest patch distributions for regions with total forest area $> 10^7 \text{ km}^2$. Dashed horizontal lines are the means by region, with 95% confidence interval error bars estimated by bootstrap resampling. The regions are AF1: Africa mainland, EUAS1: Eurasia mainland, NA1: North America mainland, SAST1: South America subtropical and tropical, SEAS1: Southeast Asia mainland.

272 SEAS2). This confirms the criteria of using the most conservative threshold value of 40% to interpret RS_{max}
273 with regard to the fragmentation state of the forest. The frequency of RS_{max} showed bimodality (Figure
274 S10) and the dip test rejected unimodality ($D = 0.0416$, p-value = 0.0003), which also implies that RS_{max}
275 is a good index to study the fragmentation state of the forest.

276 The RS_{max} for regions with more than 10^7 km^2 of forest is shown in figure 3. South America tropical and
277 subtropical (SAST1) is the only region with an average close to 60%, the other regions are below 30%. Eurasia
278 mainland (EUAS1) has the lowest value near 20%. For regions with less total forest area (Figure S10, Table
279 S3), Great Britain (EUAS3) has the lowest proportion less than 5%, Java (OC7) and Cuba (SAST2) are
280 under 25%, while other regions such as New Guinea (OC2), Malaysia/Kalimantan (OC3), Sumatra (OC4),
281 Sulawesi (OC5) and South New Zealand (OC6) have a very high proportion (75% or more). Philippines
282 (SEAS2) seems to be a very interesting case because it seems to be under 30% until the year 2007, fluctuates
283 around 30% in years 2008-2010, then jumps near 60% in 2011-2013 and then falls again to 30%, this seems
284 an example of a transition from a fragmented state to an unfragmented one (figure S11).

285 We analyzed the distributions of fluctuations of the largest patch relative to total forest area ΔRS_{max} and
286 the fluctuations of the largest patch ΔS_{max} . Although the Akaike criteria identified different distributions
287 as the best, in most cases the Likelihood ratio test was not significant and we are not able, from these data,
288 to determine with confidence which is the best distribution. In only one case was the distribution selected
289 by the Akaike criteria confirmed as the correct model for relative and absolute fluctuations (Table S4).

290 The animations of the two largest patches (see supplementary data, largest patch gif animations) qualitatively
291 shows the nature of fluctuations and if the state of the forest is connected or not. If the largest patch is
292 always the same patch over time, the forest is probably not fragmented; this happens for regions with RS_{max}
293 of more than 40% such as AF2 (Madagascar), EUAS2 (Japan), NA5 (Newfoundland) and OC3 (Malaysia).

294 In regions with RS_{max} between 40% and 30%, the identity of the largest patch could change or stay the same
295 in time. For OC7 (Java) the largest patch changes and for AF1 (Africa mainland) it stays the same. Only
296 for EUAS1 (Eurasia mainland), we observed that the two largest patches are always the same, implying
297 that these two large patches are probably by a geographical accident but they have the same dynamics.

298 The regions with RS_{max} less than 25% (SAST2-Cuba and EUAS3-Great Britain) have an always-changing
299 largest patch reflecting their fragmented state. In the case of SEAS2 (Philippines), a transition is observed,
300 with the identity of the largest patch first variable, and then constant after 2010.

301 The results of quantile regressions are almost identical for ΔRS_{max} and ΔS_{max} (table S5). Among the biggest
302 regions, Africa (AF1) has a similar pattern across thresholds but only the 30% threshold is significant; the

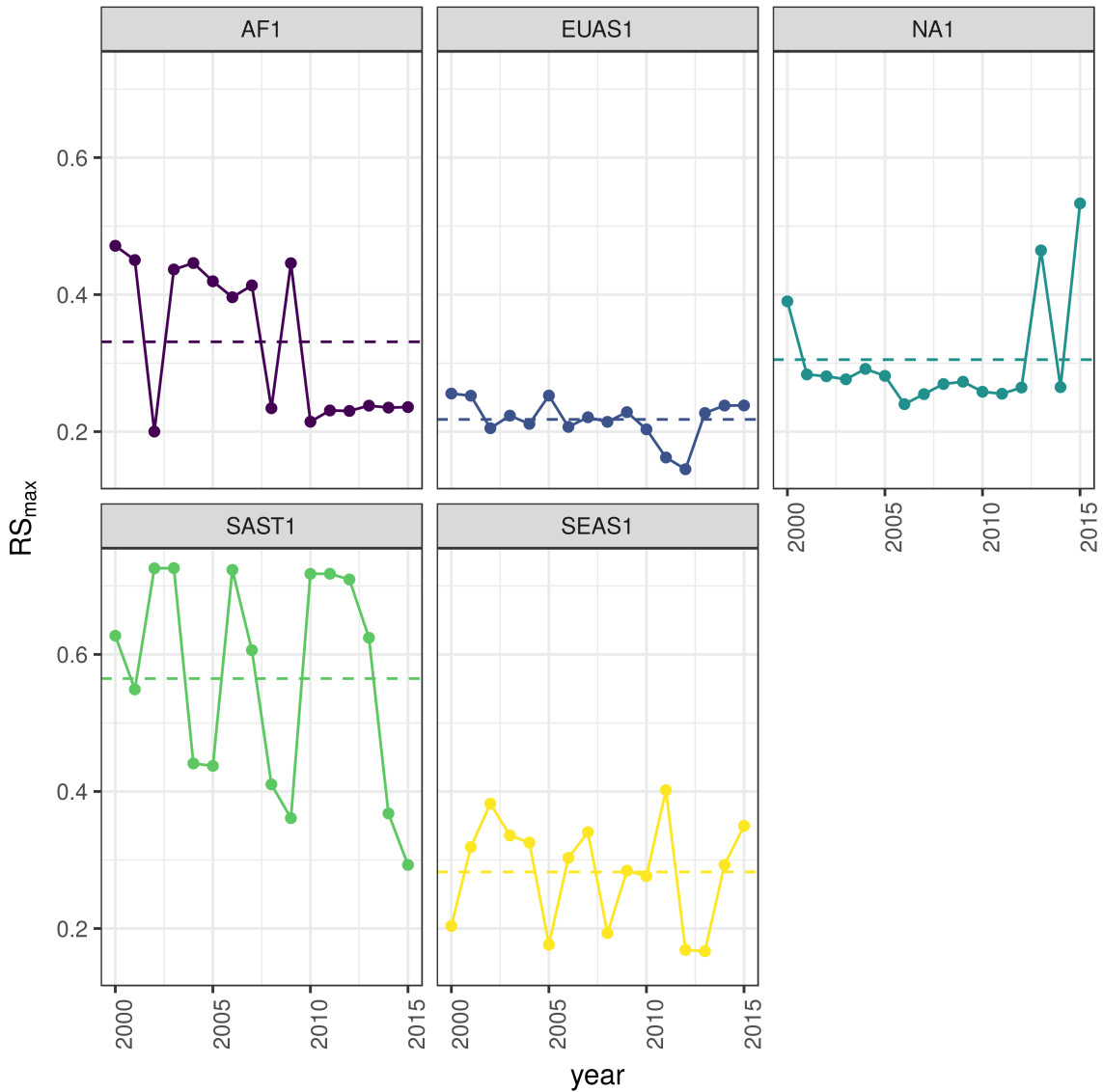


Figure 3: Largest patch proportion relative to total forest area RS_{max} , for regions with total forest area $> 10^7 \text{ km}^2$. We show here the RS_{max} calculated using a threshold of 40% of forest in each pixel to determine patches. Dashed lines are averages across time. The regions are AF1: Africa mainland, EUAS1: Eurasia mainland, NA1: North America mainland, SAST1: South America tropical and subtropical, SEAS1: Southeast Asia mainland.

303 upper and lower quantiles have significant negative slopes, but the lower quantile slope is lower, implying
304 that negative fluctuations and variance are increasing (Figure 4). Eurasia mainland (EUAS1) has significant
305 slopes at 20%, 30% and 40% thresholds but the patterns are different at 20% variance is decreasing, at
306 30% and 40% only is increasing. Thus the variation of the densest portion of the largest patch is increasing
307 within a limited range. North America mainland (NA1) exhibits the same pattern at 20%, 25% and 30%
308 thresholds: a significant lower quantile with positive slope, implying decreasing variance. South America
309 tropical and subtropical (SAST1) have significant lower quantile with a negative slope at 25% and 30%
310 thresholds indicating an increase in variance. SEAS1 has an upper quantile with positive slope significant
311 for 25% threshold, also indicating an increasing variance. The other regions, with forest area smaller than
312 10^7 km^2 are shown in figure S11 and table S5. Philippines (SEAS2) is an interesting case: the slopes of lower
313 quantiles are positive for thresholds 20% and 25%, and the upper quantile slopes are positive for thresholds
314 30% and 40%; thus variance is decreasing at 20%-25% and increasing at 30%-40%.

315 The conditions that indicate that a region is near a critical fragmentation threshold are that patch size
316 distributions follow a power law; variance of ΔRS_{max} is increasing in time, and skewness is negative. All
317 these conditions must happen at the same time at least for one threshold. When the threshold is higher more
318 dense regions of the forest are at risk. This happens for Africa mainland (AF1), Eurasia mainland(EUAS1),
319 Japan (EUAS2), Australia mainland (OC1), Malaysia/Kalimantan (OC3), Sumatra (OC4), South America
320 tropical & subtropical (SAST1), Cuba (SAST2), Southeast Asia, Mainland (SEAS1).

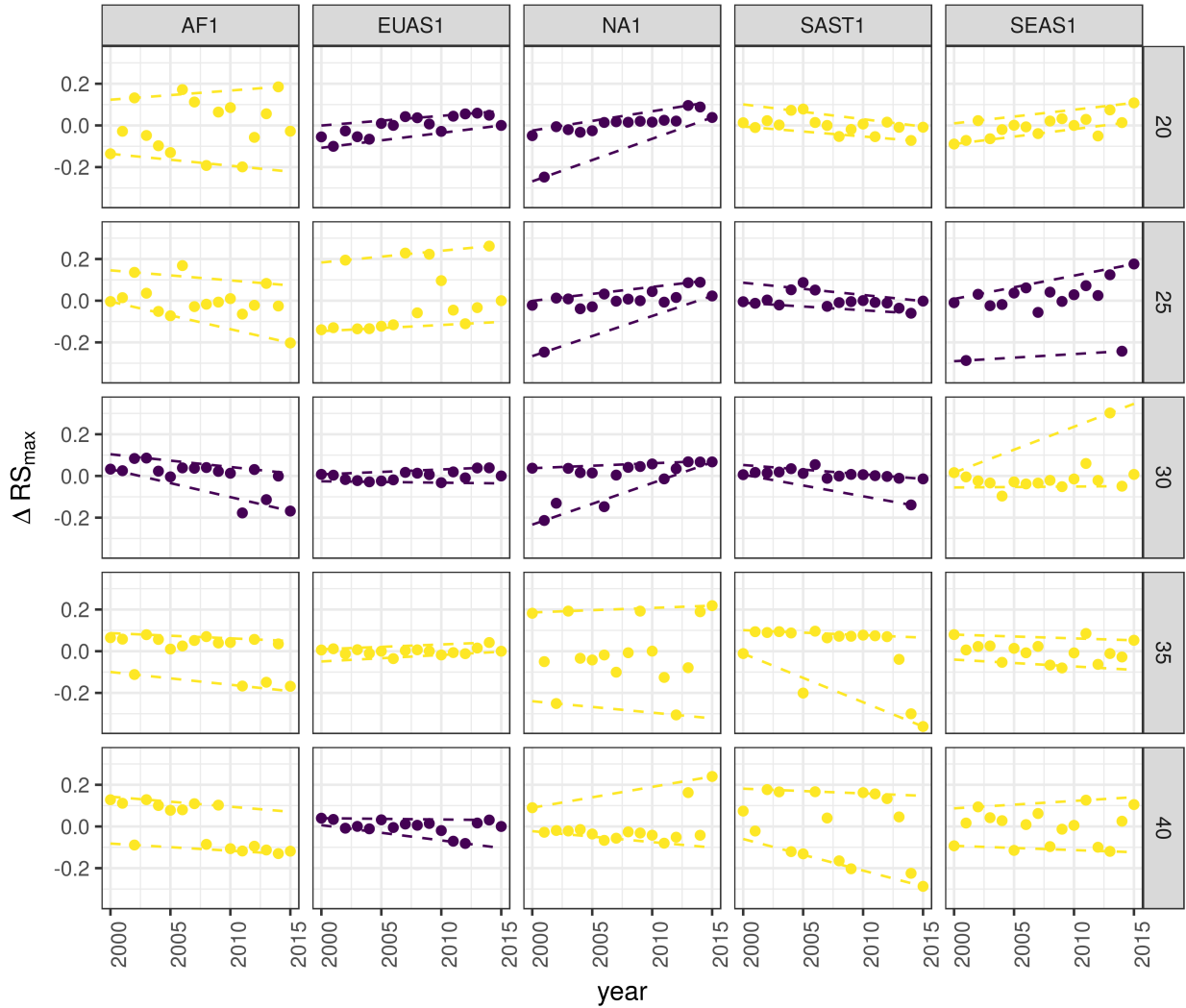


Figure 4: Largest patch fluctuations for regions with total forest area $> 10^7 \text{ km}^2$ across years. The patch sizes are relative to the total forest area of the same year. Dashed lines are 90% and 10% quantile regressions, to show if fluctuations were increasing; purple (dark) panels have significant slopes. The regions are AF1: Africa mainland, EUAS1: Eurasia mainland, NA1: North America mainland, SAST1: South America tropical and subtropical, SEAS1: Southeast Asia mainland.

Table 1: Regions and indicators of closeness to a critical fragmentation point. Where: RS_{max} is the largest patch divided by the total forest area; Threshold is the value used to calculate patches from the MODIS VCF pixels; ΔRS_{max} are the fluctuations of RS_{max} around the mean and the increase or decrease in the variance was estimated using quantile regressions; skewness was calculated for RS_{max} . NS means the results were non-significant. The conditions that determine the closeness to a fragmentation point are: increasing variance of ΔRS_{max} and negative skewness. RS_{max} indicates if the forest is unfragmented (>0.6) or fragmented (<0.3).

Region	Description	RS_{max}	Threshold	Variance of ΔRS_{max}	Skewness
AF1	Africa mainland	0.33	30	Increase	-1.4653
AF2	Madagascar	0.48	20	Increase	0.7226
EUAS1	Eurasia, mainland	0.22	20	Decrease	-0.4814
EUAS1			30	Increase	0.3113
EUAS1			40	Increase	-1.2790
EUAS2	Japan	0.94	35	Increase	-0.3913
EUAS2			40	Increase	-0.5030
EUAS3	Great Britain	0.03	40	NS	
NA1	North America, mainland	0.31	20	Decrease	-2.2895
NA1			25	Decrease	-2.4465
NA1			30	Decrease	-1.6340
NA5	Newfoundland	0.54	40	NS	
OC1	Australia, Mainland	0.36	30	Increase	0.0920
OC1			35	Increase	-0.8033
OC2	New Guinea	0.96	25	Decrease	-0.1003
OC2			30	Decrease	0.1214
OC2			35	Decrease	-0.0124
OC3	Malaysia/Kalimantan	0.92	35	Increase	-1.0147
OC3			40	Increase	-1.5649
OC4	Sumatra	0.84	20	Increase	-1.3846
OC4			25	Increase	-0.5887
OC4			30	Increase	-1.4226
OC5	Sulawesi	0.82	40	NS	
OC6	New Zealand South Island	0.75	40	Increase	0.3553
OC7	Java	0.16	40	NS	
OC8	New Zealand North Island	0.64	40	NS	
SAST1	South America, Tropical and Subtropical forest	0.56	25	Increase	1.0519
SAST1			30	Increase	-2.7216
SAST2	Cuba	0.15	20	Increase	0.5049
SAST2			25	Increase	1.7263
SAST2			30	Increase	0.1665
SAST2			40	Increase	-0.5401
SAT1	South America, Temperate forest	0.54	25	Decrease	0.1483
SAT1			30	Decrease	-1.6059
SAT1			35	Decrease	-1.3809
SEAS1	Southeast Asia, Mainland	0.28	25	Increase	-1.3328
SEAS2	Philippines	0.33	20	Decrease	-1.6373
SEAS2			25	Decrease	-0.6648
SEAS2			30	Increase	0.1517
SEAS2			40	Increase	1.5996

Region	Description	RS_{max}	Threshold	Variance of ΔRS_{max}	Skewness
--------	-------------	------------	-----------	-------------------------------	----------

321 Discussion

322 We found that the forest patch distribution of all regions of the world, spanning tropical rainforests, boreal
 323 and temperate forests, followed power laws spanning seven orders of magnitude. Power laws have previously
 324 been found for several kinds of vegetation, but never at global scales as in this study. Moreover, the range
 325 of the estimated power law exponents is relatively narrow (1.90 - 2.01), even though we tested a variety
 326 of different thresholds levels. This suggests the existence of one unifying mechanism, or perhaps different
 327 mechanisms that act in the same way in different regions, affecting forest spatial structure and dynamics.

328 Several mechanisms have been proposed for the emergence of power laws in forests. The first is related self
 329 organized criticality (SOC), when the system is driven by its internal dynamics to a critical state; this has
 330 been suggested mainly for fire-driven forests (Zinck & Grimm 2009; Hantson *et al.* 2015). Real ecosystems
 331 do not seem to meet the requirements of SOC dynamics (Pueyo *et al.* 2010; McKenzie & Kennedy 2012),
 332 however, because they have both endogenous and exogenous controls, are non-homogeneous, and do not
 333 have a separation of time scales (Solé *et al.* 2002; Solé & Bascompte 2006). A second possible mechanism,
 334 suggested by Pueyo *et al.* (2010), is isotropic percolation: when a system is near the critical point, the power
 335 law structures arise. This is equivalent to the random forest model that we explained previously, and requires
 336 the tuning of an external environmental condition to carry the system to this point. We did not expect forest
 337 growth to be a random process at local scales, but it is possible that combinations of factors cancel out to
 338 produce seemingly random forest dynamics at large scales. This has been suggested as a mechanism for the
 339 observed power laws of global tropical forest at year 2000 (Taubert *et al.* 2018). In this case we should have
 340 observed power laws in a limited set of situations that coincide with a critical point, but instead we observed
 341 pervasive power law distributions. Thus isotropic percolation does not seem likely to be the mechanism that
 342 produces the observed distributions.

343 A third possible mechanism is facilitation (Manor & Shnerb 2008; Irvine *et al.* 2016): a patch surrounded
 344 by forest will have a smaller probability of being deforested or degraded than an isolated patch. The model
 345 of Scanlon *et al.* (2007) showed an $\alpha = 1.34$ which is different from our results (1.90 - 2.01 range). Another
 346 model but with three states (tree/non-tree/degraded), including local facilitation and grazing, was also used
 347 to obtain power laws patch distributions without external tuning, and exhibited deviations from power laws
 348 at high grazing pressures (Kéfi *et al.* 2007). The values of the power law exponent α obtained for this model

349 are dependent on the intensity of facilitation: when facilitation is more intense the exponent is higher, but
350 the maximal values they obtained are still lower than the ones we observed. Thus an exploration of the
351 parameters of this model and simulations at a continental scale will be needed to find if this is a plausible
352 mechanism.

353 It has been suggested that a combination of spatial and temporal indicators could more reliably detect critical
354 transitions (Kéfi *et al.* 2014). In this study, we combined five criteria to evaluate the closeness of the system
355 to a fragmentation threshold. Two of them were spatial: the forest patch size distribution, and the proportion
356 of the largest patch relative to total forest area RS_{max} . The other three were the distribution of temporal
357 fluctuations in the largest patch size, the trend in the variance, and the skewness of the fluctuations. One
358 of them: the distribution of temporal fluctuations ΔRS_{max} can not be applied with our temporal resolution
359 due to the difficulties of fitting and comparing heavy tailed distributions. The combination of the remaining
360 four gives us an increased degree of confidence about the system being close to a critical transition.

361 Monitoring the biggest patches using RS_{max} is also important regardless of the existence or not of critical
362 transitions. RS_{max} is relative to total forest area thus it could be used to compare regions with a different
363 extension of forests and as the total area of forest also changes with different environmental conditions,
364 e.g. this could be used to compare forest from different latitudes. Moreover, the areas covered by S_{max}
365 across regions contain most of the intact forest landscapes defined by Potapov *et al.* (2008b), and thus
366 RS_{max} is a relatively simple way to evaluate the risk in these areas.

367 South America tropical and subtropical (SAST1), Southeast Asia mainland (SEAS1) and Africa mainland
368 (AF1) met all criteria at least for one threshold; these regions generally experience the biggest rates of
369 deforestation with a significant increase in loss of forest (Hansen *et al.* 2013). From our point of view the
370 most critical region is Southeast Asia, because the proportion of the largest patch relative to total forest
371 area RS_{max} was 28%. This suggests that Southeast Asia's forests are the most fragmented, and thus its
372 flora and fauna the most endangered. Due to the criteria we adopted to define regions, we could not detect
373 the effect of conservation policies applied at a country level, e.g. the Natural Forest Conservation Program
374 in China, which has produced an 1.6% increase in forest cover and net primary productivity over the last 20
375 years (Viña *et al.* 2016). Indonesia and Malaysia (OC3) both are countries with hight deforestation rates
376 (Hansen *et al.* 2013); Sumatra (OC4) is the biggest island of Indonesia and where most deforestation occurs.
377 Both regions show a high RS_{max} greater than 60%, and thus the forest is in an unfragmented state, but
378 they met all other criteria, meaning that they are approaching a transition if the actual deforestation rates
379 continue.

380 The Eurasian mainland region (EUAS1) is an extensive area with mainly temperate and boreal forest, and a
381 combination of forest loss due to fire (Potapov *et al.* 2008a) and forestry. The biggest country is Russia that
382 experienced the biggest rate of forest loss of all countries, but here in the zone of coniferous forest the the
383 largest gain is observed due to agricultural abandonment (Prishchepov *et al.* 2013). The loss is maximum
384 at the most dense areas of forest (Hansen *et al.* 2013, Table S3), this coincides with our analysis that detect
385 an increasing risk at denser forest. This region also has a relatively low RS_{max} that means is probably near
386 a fragmented state. A region that is similar in forest composition to EAUS1 is North America (NA1); the
387 two main countries involved, United States and Canada, have forest dynamics mainly influenced by fire and
388 forestry, with both regions are extensively managed for industrial wood production. North America has a
389 higher RS_{max} than Eurasia and a positive skewness that excludes it from being near a critical transition. A
390 possible explanation of this is that in Russia after the collapse of the Soviet Union harvest was lower due to
391 agricultural abandonment but illegal overharvesting of high valued stands has increased in recent decades
392 (Gauthier *et al.* 2015).

393 The analysis of RS_{max} reveals that the island of Philippines (SEAS2) seems to be an example of a critical
394 transition from an unconnected to a connected state, i.e. from a state with high fluctuations and low RS_{max}
395 to a state with low fluctuations and high RS_{max} . If we observe this pattern backwards in time, the decrease
396 in variance become an increase, and negative skewness is constant, and thus the region exhibits the criteria
397 of a critical transition (Table 1, Figure S12). The actual pattern of transition to an unfragmented state
398 could be the result of an active intervention of the government promoting conservation and rehabilitation
399 of protected areas, ban of logging old-growth forest, reforestation of barren areas, community-based forestry
400 activities, and sustainable forest management in the country's production forest (Lasco *et al.* 2008). This
401 confirms that the early warning indicators proposed here work in the correct direction. An important caveat
402 is that the MODIS dataset does not detect if native forest is replaced by agroindustrial tree plantations like
403 oil palms, that are among the main drivers of deforestation in this area (Malhi *et al.* 2014). To improve
404 the estimation of forest patches, data sets as the MODIS cropland probability and others about land use,
405 protected areas, forest type, should be incorporated (Hansen *et al.* 2014; Sexton *et al.* 2015).

406 Deforestation and fragmentation are closely related. At low levels of habitat reduction species population
407 will decline proportionally; this can happen even when the habitat fragments retain connectivity. As habitat
408 reduction continues, the critical threshold is approached and connectivity will have large fluctuations (Brook
409 *et al.* 2013). This could trigger several negative synergistic effects: population fluctuations and the possibility
410 of extinctions will rise, increasing patch isolation and decreasing connectivity (Brook *et al.* 2013). This
411 positive feedback mechanism will be enhanced when the fragmentation threshold is reached, resulting in the

loss of most habitat specialist species at a landscape scale (Pardini *et al.* 2010). Some authors have argued that since species have heterogeneous responses to habitat loss and fragmentation, and biotic dispersal is limited, the importance of thresholds is restricted to local scales or even that its existence is questionable (Brook *et al.* 2013). Fragmentation is by definition a local process that at some point produces emergent phenomena over the entire landscape, even if the area considered is infinite (Oborny *et al.* 2005). If a forest is already in a fragmented state, a second critical transition from forest to non-forest could happen: the desertification transition (Corrado *et al.* 2014). Considering the actual trends of habitat loss, and studying the dynamics of non-forest patches—instead of the forest patches as we did here—the risk of this kind of transition could be estimated. The simple models proposed previously could also be used to estimate if these thresholds are likely to be continuous and reversible or discontinuous and often irreversible (Weissmann & Shnerb 2016), and the degree of protection (e.g. using the set-asides strategy Banks-Leite *et al.* (2014)) that would be necessary to stop this trend.

The effectiveness of landscape management is related to the degree of fragmentation, and the criteria to direct reforestation efforts could be focused on regions near a transition (Oborny *et al.* 2007). Regions that are in an unconnected state require large efforts to recover a connected state, but regions that are near a transition could be easily pushed to a connected state; feedbacks due to facilitation mechanisms might help to maintain this state. Crossing the fragmentation critical point in forests could have negative effects on biodiversity and ecosystem services (Haddad *et al.* 2015), but it could also produce feedback loops at different levels of the biological hierarchy. This means that a critical transition produced at a continental scale could have effects at the level of communities, food webs, populations, phenotypes and genotypes (Barnosky *et al.* 2012). All these effects interact with climate change, thus there is a potential production of cascading effects that could lead to an abrupt climate change with potentially large ecological and economic impact (Alley *et al.* 2003).

Therefore, even if critical thresholds are reached only in some forest regions at a continental scale, a cascading effect with global consequences could still be produced (Reyer *et al.* 2015). The risk of such event will be higher if the dynamics of separate continental regions are coupled (Lenton & Williams 2013). At least three of the regions defined here are considered tipping elements of the earth climate system that could be triggered during this century (Lenton *et al.* 2008). These were defined as policy relevant tipping elements so that political decisions could determine whether the critical value is reached or not. Thus the criteria proposed here could be used as a more sensitive system to evaluate the closeness of a tipping point at a continental scale. Further improvements will produce quantitative predictions about the temporal horizon where these critical transitions could produce significant changes in the studied systems.

⁴⁴³ **Supporting information**

⁴⁴⁴ **Appendix**

⁴⁴⁵ *Table S1:* Mean power-law exponent and Bootstrapped 95% confidence intervals by threshold.

⁴⁴⁶ *Table S2:* Mean power-law exponent and Bootstrapped 95% confidence intervals across thresholds by region
⁴⁴⁷ and year.

⁴⁴⁸ *Table S3:* Mean total patch area; largest patch S_{max} in km²; largest patch relative to total patch area RS_{max}
⁴⁴⁹ and 95% bootstrapped confidence interval of RS_{max} , by region and thresholds, averaged across years

⁴⁵⁰ *Table S4:* Model selection for distributions of fluctuation of largest patch ΔS_{max} and largest patch relative
⁴⁵¹ to total forest area ΔRS_{max} .

⁴⁵² *Table S5:* Quantil regressions of the fluctuations of the largest patch vs year, for 10% and 90% quantils at
⁴⁵³ different pixel thresholds.

⁴⁵⁴ *Table S6:* Unbiased estimation of Skewness of fluctuations of the largest patch ΔS_{max} and fluctuations
⁴⁵⁵ relative to total forest area ΔRS_{max} .

⁴⁵⁶ *Figure S1:* Regions for Africa: Mainland (AF1), Madagascar (AF2).

⁴⁵⁷ *Figure S2:* Regions for Eurasia: Mainland (EUAS1), Japan (EUAS2), Great Britain (EUAS3).

⁴⁵⁸ *Figure S3:* Regions for North America: Mainland (NA1), Newfoundland (NA5).

⁴⁵⁹ *Figure S4:* Regions for Australia and islands: Australia mainland (OC1), New Guinea (OC2),
⁴⁶⁰ Malaysia/Kalimantan (OC3), Sumatra (OC4), Sulawesi (OC5), New Zealand south island (OC6),
⁴⁶¹ Java (OC7), New Zealand north island (OC8).

⁴⁶² *Figure S5:* Regions for South America: Tropical and subtropical forest up to Mexico (SAST1), Cuba
⁴⁶³ (SAST2), South America Temperate forest (SAT1).

⁴⁶⁴ *Figure S6:* Regions for Southeast Asia: Mainland (SEAS1), Philippines (SEAS2).

⁴⁶⁵ *Figure S7:* Proportion of best models selected for patch size distributions using the Akaike criterion.

⁴⁶⁶ *Figure S8:* Power law exponents for forest patch distributions by year for all regions.

⁴⁶⁷ *Figure S9:* Average largest patch relative to total forest area RS_{max} by threshold, for all regions.

⁴⁶⁸ *Figure s10:* Frequency distribution of Largest patch proportion relative to total forest area RS_{max} calculated
⁴⁶⁹ using a threshold of 40%.

470 *Figure S11:* Largest patch relative to total forest area RS_{max} by year at 40% threshold, for regions with
471 total forest area less than 10^7 km^2 .

472 *Figure S12:* Fluctuations of largest patch relative to total forest area RS_{max} for regions with total forest
473 area less than 10^7 km^2 by year and threshold.

474 Data Accessibility

475 The MODIS VCF product is freely available from NASA at <https://search.earthdata.nasa.gov/>. Csv text file
476 with model fits for patch size distribution, and model selection for all the regions; Gif Animations of a forest
477 model percolation; Gif animations of largest patches; patch size files for all years and regions used here; and all
478 the R, Python and Matlab scripts are available at figshare <http://dx.doi.org/10.6084/m9.figshare.4263905>.

479 Acknowledgments

480 LAS and SRD are grateful to the National University of General Sarmiento for financial support. We want to
481 thank to Jordi Bascompte, Nara Guisoni, Fernando Momo, and two anonymous reviewers for their comments
482 and discussions that greatly improved the manuscript. This work was partially supported by a grant from
483 CONICET (PIO 144-20140100035-CO).

484 References

- 485 Alley, R.B., Marotzke, J., Nordhaus, W.D., Overpeck, J.T., Peteet, D.M. & Pielke, R.A. *et al.* (2003).
486 Abrupt Climate Change. *Science*, 299, 2005–2010.
- 487 Allington, G.R.H. & Valone, T.J. (2010). Reversal of desertification: The role of physical and chemical soil
488 properties. *Journal of Arid Environments*, 74, 973–977.
- 489 Alstott, J., Bullmore, E. & Plenz, D. (2014). powerlaw: A Python Package for Analysis of Heavy-Tailed
490 Distributions. *PLOS ONE*, 9, e85777.
- 491 Angelsen, A. (2010). Policies for reduced deforestation and their impact on agricultural production. *Pro-*
492 *ceedings of the National Academy of Sciences*, 107, 19639–19644.
- 493 Banks-Leite, C., Pardini, R., Tambosi, L.R., Pearse, W.D., Bueno, A.A. & Bruscagin, R.T. *et al.* (2014).
494 Using ecological thresholds to evaluate the costs and benefits of set-asides in a biodiversity hotspot. *Science*,

- 495 345, 1041–1045.
- 496 Barnosky, A.D., Hadly, E.A., Bascompte, J., Berlow, E.L., Brown, J.H. & Fortelius, M. *et al.* (2012).
497 Approaching a state shift in Earth’s biosphere. *Nature*, 486, 52–58.
- 498 Bascompte, J. & Solé, R.V. (1996). Habitat fragmentation and extinction thresholds in spatially explicit
499 models. *Journal of Animal Ecology*, 65, 465–473.
- 500 Bazant, M.Z. (2000). Largest cluster in subcritical percolation. *Physical Review E*, 62, 1660–1669.
- 501 Belward, A.S. (1996). *The IGBP-DIS Global 1 Km Land Cover Data Set “DISCover”: Proposal and*
502 *Implementation Plans : Report of the Land Recover Working Group of IGBP-DIS*. IGBP-dis working paper.
503 IGBP-DIS Office.
- 504 Benedetti-Cecchi, L., Tamburello, L., Maggi, E. & Bulleri, F. (2015). Experimental Perturbations Modify
505 the Performance of Early Warning Indicators of Regime Shift. *Current biology*, 25, 1867–1872.
- 506 Bestelmeyer, B.T., Duniway, M.C., James, D.K., Burkett, L.M. & Havstad, K.M. (2013). A test of critical
507 thresholds and their indicators in a desertification-prone ecosystem: more resilience than we thought. *Ecology*
508 *Letters*, 16, 339–345.
- 509 Bestelmeyer, B.T., Ellison, A.M., Fraser, W.R., Gorman, K.B., Holbrook, S.J. & Laney, C.M. *et al.* (2011).
510 Analysis of abrupt transitions in ecological systems. *Ecosphere*, 2, 129.
- 511 Boettiger, C. & Hastings, A. (2012). Quantifying limits to detection of early warning for critical transitions.
512 *Journal of The Royal Society Interface*, 9, 2527–2539.
- 513 Bonan, G.B. (2008). Forests and Climate Change: Forcings, Feedbacks, and the Climate Benefits of Forests.
514 *Science*, 320, 1444–1449.
- 515 Botet, R. & Ploszajczak, M. (2004). Correlations in Finite Systems and Their Universal Scaling Properties.
516 In: *Nonequilibrium physics at short time scales: Formation of correlations* (ed. Morawetz, K.). Springer-
517 Verlag, Berlin Heidelberg, pp. 445–466.
- 518 Brook, B.W., Ellis, E.C., Perring, M.P., Mackay, A.W. & Blomqvist, L. (2013). Does the terrestrial biosphere
519 have planetary tipping points? *Trends in Ecology & Evolution*.
- 520 Burnham, K. & Anderson, D.R. (2002). *Model selection and multi-model inference: A practical information-*
521 *theoretic approach*. 2nd. edn. Springer-Verlag, New York.
- 522 Canfield, D.E., Glazer, A.N. & Falkowski, P.G. (2010). The Evolution and Future of Earth’s Nitrogen Cycle.

- 523 Carpenter, S.R., Cole, J.J., Pace, M.L., Batt, R., Brock, W.A. & Cline, T. *et al.* (2011). Early Warnings of
524 Regime Shifts: A Whole-Ecosystem Experiment. *Science*, 332, 1079–1082.
- 525
- 526 Clauset, A., Shalizi, C. & Newman, M. (2009). Power-Law Distributions in Empirical Data. *SIAM Review*,
527 51, 661–703.
- 528 Corrado, R., Cherubini, A.M. & Pennetta, C. (2014). Early warning signals of desertification transitions in
529 semiarid ecosystems. *Physical Review E - Statistical, Nonlinear, and Soft Matter Physics*, 90, 62705.
- 530 Crawley, M.J. (2012). *The R Book*. 2nd. edn. Wiley, Hoboken, NJ, USA.
- 531 Crowther, T.W., Glick, H.B., Covey, K.R., Bettigole, C., Maynard, D.S. & Thomas, S.M. *et al.* (2015).
532 Mapping tree density at a global scale. *Nature*, 525, 201–205.
- 533 Dai, L., Vorselen, D., Korolev, K.S. & Gore, J. (2012). Generic Indicators for Loss of Resilience Before a
534 Tipping Point Leading to Population Collapse. *Science*, 336, 1175–1177.
- 535 DiMiceli, C., Carroll, M., Sohlberg, R., Huang, C., Hansen, M. & Townshend, J. (2015). Annual Global
536 Automated MODIS Vegetation Continuous Fields (MOD44B) at 250 m Spatial Resolution for Data Years
537 Beginning Day 65, 2000 - 2014, Collection 051 Percent Tree Cover, University of Maryland, College Park,
538 MD, USA.
- 539 Drake, J.M. & Griffen, B.D. (2010). Early warning signals of extinction in deteriorating environments.
540 *Nature*, 467, 456–459.
- 541 Efron, B. & Tibshirani, R.J. (1994). *An Introduction to the Bootstrap*. Chapman & hall/crc monographs on
542 statistics & applied probability. Taylor & Francis, New York.
- 543 Filotas, E., Parrott, L., Burton, P.J., Chazdon, R.L., Coates, K.D. & Coll, L. *et al.* (2014). Viewing forests
544 through the lens of complex systems science. *Ecosphere*, 5, 1–23.
- 545 Foley, J.A., Ramankutty, N., Brauman, K.A., Cassidy, E.S., Gerber, J.S. & Johnston, M. *et al.* (2011).
546 Solutions for a cultivated planet. *Nature*, 478, 337–342.
- 547 Fung, T., O'Dwyer, J.P., Rahman, K.A., Fletcher, C.D. & Chisholm, R.A. (2016). Reproducing static and
548 dynamic biodiversity patterns in tropical forests: the critical role of environmental variance. *Ecology*, 97,
549 1207–1217.
- 550 Gardner, R.H. & Urban, D.L. (2007). Neutral models for testing landscape hypotheses. *Landscape Ecology*,

- 551 22, 15–29.
- 552 Gastner, M.T., Oborny, B., Zimmermann, D.K. & Pruessner, G. (2009). Transition from Connected to Frag-
553 mented Vegetation across an Environmental Gradient: Scaling Laws in Ecotone Geometry. *The American
554 Naturalist*, 174, E23–E39.
- 555 Gauthier, S., Bernier, P., Kuuluvainen, T., Shvidenko, A.Z. & Schepaschenko, D.G. (2015). Boreal forest
556 health and global change. *Science*, 349, 819 LP–822.
- 557 Gilman, S.E., Urban, M.C., Tewksbury, J., Gilchrist, G.W. & Holt, R.D. (2010). A framework for community
558 interactions under climate change. *Trends in Ecology & Evolution*, 25, 325–331.
- 559 Goldstein, M.L., Morris, S.A. & Yen, G.G. (2004). Problems with fitting to the power-law distribution. *The
560 European Physical Journal B - Condensed Matter and Complex Systems*, 41, 255–258.
- 561 Haddad, N.M., Brudvig, L.a., Clobert, J., Davies, K.F., Gonzalez, A. & Holt, R.D. *et al.* (2015). Habitat
562 fragmentation and its lasting impact on Earth’s ecosystems. *Science Advances*, 1, 1–9.
- 563 Hansen, M., Potapov, P., Margono, B., Stehman, S., Turubanova, S. & Tyukavina, A. (2014). Response to
564 Comment on “High-resolution global maps of 21st-century forest cover change”. *Science*, 344, 981.
- 565 Hansen, M.C., Potapov, P.V., Moore, R., Hancher, M., Turubanova, S.A. & Tyukavina, A. *et al.* (2013).
566 High-Resolution Global Maps of 21st-Century Forest Cover Change. *Science*, 342, 850–853.
- 567 Hantson, S., Pueyo, S. & Chuvieco, E. (2015). Global fire size distribution is driven by human impact and
568 climate. *Global Ecology and Biogeography*, 24, 77–86.
- 569 Harris, T.E. (1974). Contact interactions on a lattice. *The Annals of Probability*, 2, 969–988.
- 570 Hartigan, J.A. & Hartigan, P.M. (1985). The Dip Test of Unimodality. *The Annals of Statistics*, 13, 70–84.
- 571 Hastings, A. & Wysham, D.B. (2010). Regime shifts in ecological systems can occur with no warning. *Ecology
572 Letters*, 13, 464–472.
- 573 He, F. & Hubbell, S. (2003). Percolation Theory for the Distribution and Abundance of Species. *Physical
574 Review Letters*, 91, 198103.
- 575 Hinrichsen, H. (2000). Non-equilibrium critical phenomena and phase transitions into absorbing states.
576 *Advances in Physics*, 49, 815–958.
- 577 Hirota, M., Holmgren, M., Nes, E.H.V. & Scheffer, M. (2011). Global Resilience of Tropical Forest and

- 578 Savanna to Critical Transitions. *Science*, 334, 232–235.
- 579 Irvine, M.A., Bull, J.C. & Keeling, M.J. (2016). Aggregation dynamics explain vegetation patch-size distri-
580 butions. *Theoretical Population Biology*, 108, 70–74.
- 581 Keitt, T.H., Urban, D.L. & Milne, B.T. (1997). Detecting critical scales in fragmented landscapes. *Conser-
582 vation Ecology*, 1, 4.
- 583 Kéfi, S., Guttal, V., Brock, W.A., Carpenter, S.R., Ellison, A.M. & Livina, V.N. *et al.* (2014). Early
584 Warning Signals of Ecological Transitions: Methods for Spatial Patterns. *PLoS ONE*, 9, e92097.
- 585 Kéfi, S., Rietkerk, M., Alados, C.L., Pueyo, Y., Papanastasis, V.P. & ElAich, A. *et al.* (2007). Spatial
586 vegetation patterns and imminent desertification in Mediterranean arid ecosystems. *Nature*, 449, 213–217.
- 587 Kitzberger, T., Aráoz, E., Gowda, J.H., Mermoz, M. & Morales, J.M. (2012). Decreases in Fire Spread Prob-
588 ability with Forest Age Promotes Alternative Community States, Reduced Resilience to Climate Variability
589 and Large Fire Regime Shifts. *Ecosystems*, 15, 97–112.
- 590 Koenker, R. (2016). quantreg: Quantile Regression.
- 591 Lasco, R.D., Pulhin, F.B., Cruz, R.V.O., Pulhin, J.M., Roy, S.S.N. & Sanchez, P.A.J. (2008). Forest
592 responses to changing rainfall in the Philippines. In: *Climate change and vulnerability* (eds. Leary, N.,
593 Conde, C. & Kulkarni, J.). Earthscan, London, pp. 49–66.
- 594 Leibold, M.A. & Norberg, J. (2004). Biodiversity in metacommunities: Plankton as complex adaptive
595 systems? *Limnology and Oceanography*, 49, 1278–1289.
- 596 Lenton, T.M. & Williams, H.T.P. (2013). On the origin of planetary-scale tipping points. *Trends in Ecology
597 & Evolution*, 28, 380–382.
- 598 Lenton, T.M., Held, H., Kriegler, E., Hall, J.W., Lucht, W. & Rahmstorf, S. *et al.* (2008). Tipping elements
599 in the Earth's climate system. *Proceedings of the National Academy of Sciences*, 105, 1786–1793.
- 600 Limpert, E., Stahel, W.A. & Abbt, M. (2001). Log-normal Distributions across the Sciences: Keys and
601 CluesOn the charms of statistics, and how mechanical models resembling gambling machines offer a link to
602 a handy way to characterize log-normal distributions, which can provide deeper insight into var. *BioScience*,
603 51, 341–352.
- 604 Loehle, C., Li, B.-L. & Sundell, R.C. (1996). Forest spread and phase transitions at forest-prairie ecotones
605 in Kansas, U.S.A. *Landscape Ecology*, 11, 225–235.
- 606 Malhi, Y., Gardner, T.A., Goldsmith, G.R., Silman, M.R. & Zelazowski, P. (2014). Tropical Forests in the

- 607 Anthropocene. *Annual Review of Environment and Resources*, 39, 125–159.
- 608 609 Manor, A. & Shnerb, N.M. (2008). Origin of pareto-like spatial distributions in ecosystems. *Physical Review Letters*, 101, 268104.
- 610 611 McKenzie, D. & Kennedy, M.C. (2012). Power laws reveal phase transitions in landscape controls of fire regimes. *Nat Commun*, 3, 726.
- 612 613 614 Mitchell, M.G.E., Suarez-Castro, A.F., Martinez-Harms, M., Maron, M., McAlpine, C. & Gaston, K.J. *et al.* (2015). Reframing landscape fragmentation's effects on ecosystem services. *Trends in Ecology & Evolution*, 30, 190–198.
- 615 616 Naito, A.T. & Cairns, D.M. (2015). Patterns of shrub expansion in Alaskan arctic river corridors suggest phase transition. *Ecology and Evolution*, 5, 87–101.
- 617 618 Newman, M.E.J. (2005). Power laws, Pareto distributions and Zipf's law. *Contemporary Physics*, 46, 323–351.
- 619 620 Oborny, B., Meszéna, G. & Szabó, G. (2005). Dynamics of Populations on the Verge of Extinction. *Oikos*, 109, 291–296.
- 621 622 Oborny, B., Szabó, G. & Meszéna, G. (2007). Survival of species in patchy landscapes: percolation in space and time. In: *Scaling biodiversity*. Cambridge University Press, pp. 409–440.
- 623 624 Ochoa-Quintero, J.M., Gardner, T.A., Rosa, I., de Barros Ferraz, S.F. & Sutherland, W.J. (2015). Thresholds of species loss in Amazonian deforestation frontier landscapes. *Conservation Biology*, 29, 440–451.
- 625 626 Ódor, G. (2004). Universality classes in nonequilibrium lattice systems. *Reviews of Modern Physics*, 76, 663–724.
- 627 628 Pardini, R., Bueno, A. de A., Gardner, T.A., Prado, P.I. & Metzger, J.P. (2010). Beyond the Fragmentation Threshold Hypothesis: Regime Shifts in Biodiversity Across Fragmented Landscapes. *PLoS ONE*, 5, e13666.
- 629 630 631 Potapov, P., Hansen, M.C., Stehman, S.V., Loveland, T.R. & Pittman, K. (2008a). Combining MODIS and Landsat imagery to estimate and map boreal forest cover loss. *Remote Sensing of Environment*, 112, 3708–3719.
- 632 633 Potapov, P., Yaroshenko, A., Turubanova, S., Dubinin, M., Laestadius, L. & Thies, C. *et al.* (2008b). Mapping the world's intact forest landscapes by remote sensing. *Ecology and Society*, 13.
- 634 Prishchepov, A.V., Müller, D., Dubinin, M., Baumann, M. & Radeloff, V.C. (2013). Determinants of

- 635 agricultural land abandonment in post-Soviet European Russia. *Land Use Policy*, 30, 873–884.
- 636 Pueyo, S., de Alencastro Graça, P.M.L., Barbosa, R.I., Cots, R., Cardona, E. & Fearnside, P.M. (2010).
637 Testing for criticality in ecosystem dynamics: the case of Amazonian rainforest and savanna fire. *Ecology
Letters*, 13, 793–802.
- 638
- 639 R Core Team. (2015). R: A Language and Environment for Statistical Computing.
- 640 Reyer, C.P.O., Rammig, A., Brouwers, N. & Langerwisch, F. (2015). Forest resilience, tipping points and
641 global change processes. *Journal of Ecology*, 103, 1–4.
- 642 Rooij, M.M.J.W. van, Nash, B., Rajaraman, S. & Holden, J.G. (2013). A Fractal Approach to Dynamic
643 Inference and Distribution Analysis. *Frontiers in Physiology*, 4.
- 644 Rudel, T.K., Coomes, O.T., Moran, E., Achard, F., Angelsen, A. & Xu, J. et al. (2005). Forest transitions:
645 towards a global understanding of land use change. *Global Environmental Change*, 15, 23–31.
- 646 Saravia, L.A. & Momo, F.R. (2018). Biodiversity collapse and early warning indicators in a spatial phase
647 transition between neutral and niche communities. *Oikos*, 127, 111–124.
- 648 Scanlon, T.M., Caylor, K.K., Levin, S.A. & Rodriguez-iturbe, I. (2007). Positive feedbacks promote power-
649 law clustering of Kalahari vegetation. *Nature*, 449, 209–212.
- 650 Scheffer, M., Bascompte, J., Brock, W.A., Brovkin, V., Carpenter, S.R. & Dakos, V. et al. (2009). Early-
651 warning signals for critical transitions. *Nature*, 461, 53–59.
- 652 Scheffer, M., Walker, B., Carpenter, S., Foley, J. a, Folke, C. & Walker, B. (2001). Catastrophic shifts in
653 ecosystems. *Nature*, 413, 591–596.
- 654 Seidler, T.G. & Plotkin, J.B. (2006). Seed Dispersal and Spatial Pattern in Tropical Trees. *PLoS Biology*,
655 4, e344.
- 656 Sexton, J.O., Noojipady, P., Song, X.-P., Feng, M., Song, D.-X. & Kim, D.-H. et al. (2015). Conservation
657 policy and the measurement of forests. *Nature Climate Change*, 6, 192–196.
- 658 Sexton, J.O., Song, X.-P., Feng, M., Noojipady, P., Anand, A. & Huang, C. et al. (2013). Global, 30-m
659 resolution continuous fields of tree cover: Landsat-based rescaling of MODIS vegetation continuous fields
660 with lidar-based estimates of error. *International Journal of Digital Earth*, 6, 427–448.
- 661 Solé, R.V. (2011). *Phase Transitions*. Primers in complex systems. Princeton University Press.
- 662 Solé, R.V. & Bascompte, J. (2006). *Self-organization in complex ecosystems*. Princeton University Press,

- 663 New Jersey, USA.
- 664 Solé, R.V., Alonso, D. & Mckane, A. (2002). Self-organized instability in complex ecosystems. *Philosophical
665 transactions of the Royal Society of London. Series B, Biological sciences*, 357, 667–681.
- 666 Solé, R.V., Alonso, D. & Saldaña, J. (2004). Habitat fragmentation and biodiversity collapse in neutral
667 communities. *Ecological Complexity*, 1, 65–75.
- 668 Solé, R.V., Bartumeus, F. & Gamarra, J.G.P. (2005). Gap percolation in rainforests. *Oikos*, 110, 177–185.
- 669 Staal, A., Dekker, S.C., Xu, C. & Nes, E.H. van. (2016). Bistability, Spatial Interaction, and the Distribution
670 of Tropical Forests and Savannas. *Ecosystems*, 19, 1080–1091.
- 671 Stauffer, D. & Aharony, A. (1994). *Introduction To Percolation Theory*. Taylor & Francis, London.
- 672 Taubert, F., Fischer, R., Groeneveld, J., Lehmann, S., Müller, M.S. & Rödig, E. et al. (2018). Global
673 patterns of tropical forest fragmentation. *Nature*.
- 674 Vasilakopoulos, P. & Marshall, C.T. (2015). Resilience and tipping points of an exploited fish population
675 over six decades. *Global Change Biology*, 21, 1834–1847.
- 676 Villa Martín, P., Bonachela, J.A. & Muñoz, M.A. (2014). Quenched disorder forbids discontinuous transitions
677 in nonequilibrium low-dimensional systems. *Physical Review E*, 89, 12145.
- 678 Villa Martín, P., Bonachela, J.A., Levin, S.A. & Muñoz, M.A. (2015). Eluding catastrophic shifts. *Proceed-
679 ings of the National Academy of Sciences*, 112, E1828–E1836.
- 680 Viña, A., McConnell, W.J., Yang, H., Xu, Z. & Liu, J. (2016). Effects of conservation policy on China's
681 forest recovery. *Science Advances*, 2, e1500965.
- 682 Vuong, Q.H. (1989). Likelihood Ratio Tests for Model Selection and Non-Nested Hypotheses. *Econometrica*,
683 57, 307–333.
- 684 Weissmann, H. & Shnerb, N.M. (2016). Predicting catastrophic shifts. *Journal of Theoretical Biology*, 397,
685 128–134.
- 686 Wuyts, B., Champneys, A.R. & House, J.I. (2017). Amazonian forest-savanna bistability and human impact.
687 *Nature Communications*, 8, 15519.
- 688 Xu, C., Hantson, S., Holmgren, M., Nes, E.H. van, Staal, A. & Scheffer, M. (2016). Remotely sensed canopy
689 height reveals three pantropical ecosystem states. *Ecology*, 97, 2518–2521.
- 690 Zhang, J.Y., Wang, Y., Zhao, X., Xie, G. & Zhang, T. (2005). Grassland recovery by protection from grazing

- 691 in a semi-arid sandy region of northern China. *New Zealand Journal of Agricultural Research*, 48, 277–284.
- 692 Zinck, R.D. & Grimm, V. (2009). Unifying wildfire models from ecology and statistical physics. *The*
- 693 *American naturalist*, 174, E170–85.